

Loss and Index Guiding in Single-Mode Proton-Implanted Holey Vertical-Cavity Surface-Emitting Lasers

Paul O. Leisher, *Student Member, IEEE*, Aaron J. Danner, *Member, IEEE*, James J. Raftery Jr., *Member, IEEE*, Dominic Siriani, and Kent D. Choquette, *Fellow, IEEE*

Abstract—Wedge-shaped holes are fabricated in the top mirror of proton-implanted vertical-cavity surface-emitting lasers (VCSELs). A radially symmetric fill factor approach is used to calculate the resulting transverse index profile. To investigate both the index confinement provided by the etched pattern and its effect on optical loss, continuous-wave (CW) and pulsed experiments are performed. Under CW operation, we show proper wedge design leads to improved fundamental-mode output power, decreased threshold, and increased efficiency. We report a significant decrease in threshold under pulsed operation for the etched device compared to an unetched device, indicating a significant reduction in diffraction loss to the fundamental mode due to strong index guiding. Single-mode output is maintained over the entire operating range of the VCSEL due to increased loss for the higher order modes.

Index Terms—Distributed Bragg reflector lasers, semiconductor lasers.

I. INTRODUCTION

VERTICAL-CAVITY surface-emitting lasers (VCSELs) are an ideal source for short-haul optical telecommunication. VCSELs provide a number of benefits over edge-emitting lasers including low cost, high volume manufacture, the capability for on-wafer testing, inherent single longitudinal mode operation, and the ability to easily fabricate large arrays. However, VCSELs tend to operate in multiple transverse modes. Single-mode laser sources are desired for high bandwidth operation of fiber optic links, sensing, and atomic clocks.

A variety of methods have been previously explored for achieving single transverse-mode operation in VCSELs. These include the incorporation of small diameter ($<3 \mu\text{m}$) oxide apertures [1], proton-implanted apertures [2], oxide/implant hybrid structures [3], surface relief etching [4], [5], photonic crystals [6]–[10], and holey structures (such as wedges) [11]. The use of photonic crystals [12] and holey wedge structures [13] in proton-implanted VCSELs has only recently been reported.

Manuscript received February 26, 2006; revised September 6, 2006. This work is supported in part by the National Science Foundation under Grant 03-35082.

P. O. Leisher, D. Siriani, and K. D. Choquette are with the Micro and Nanotechnology Laboratory, Department of Electrical and Computer Engineering, University of Illinois at Urbana-Champaign, Urbana, IL 61801 USA (e-mail: pleisher@ieec.org).

A. J. Danner was with Agilent Technologies, 109673 Singapore. He is now with Avago Technologies, 109673 Singapore.

J. J. Raftery, Jr. is with the Photonics Research Center, U.S. Military Academy, West Point, NY 10996 USA.

Digital Object Identifier 10.1109/QE.2006.882031

Using a proton implantation for electronic confinement has several advantages over the use of oxide-confinement in holey VCSELs. First, implant devices are inherently single mode at threshold [2], and only lase in a few higher order transverse modes at higher current, whereas oxide devices with similar aperture sizes are strongly index-guided from threshold to saturation [14]. Second, because thermal lensing is a weak effect, the holey structure allows the optical confinement to be decoupled from the current confinement, providing another degree of freedom which can be used for optimization of device performance. Other advantages include precise manufacturability and potentially improved modulation bandwidth.

Etching a holey structure can cause the threshold current to increase in oxide-confined devices due to increased scattering off the holes and nonoptimal overlap between the oxide and the optical mode. For proton-implanted VCSELs, the absence of higher order modes around threshold minimizes the increase in threshold current due to the holey structure. Moreover, the index confinement provided by the etched pattern can actually reduce the threshold current by reducing diffraction loss.

In this work, the index profile of an etched wedge design pattern is analyzed using a simple radially symmetric fill factor approach. A number of implant-confined holey wedge VCSELs are designed and fabricated. The CW and pulsed results from this experiment are then presented and analyzed in terms of index confinement and loss.

II. ANALYSIS

Fig. 1(a) illustrates a prototype holey wedge design pattern. The optical aperture diameter is given by R ; the total number of wedges is given by N ; the index of refraction of the air and bulk semiconductor are given by n_o and n_s , respectively; and each wedge arc subtends an angle given by θ in radians. Although modal solutions to this waveguide structure can be computed numerically using standard computation techniques, a simple model is desired. An average index of refraction as a function of radius r is derived using a radially symmetric fill-factor approach. This effective index is approximately given by

$$n(r) = \begin{cases} n_s, & r < R \\ \frac{NL}{2\pi r} n_o + \left(1 - \frac{NL}{2\pi r}\right) n_s, & r > R \end{cases}$$

where

$$L = r\theta - 2r \sin^{-1}(R/r \sin(\theta/2)) \approx (r - R)\theta. \quad (1)$$

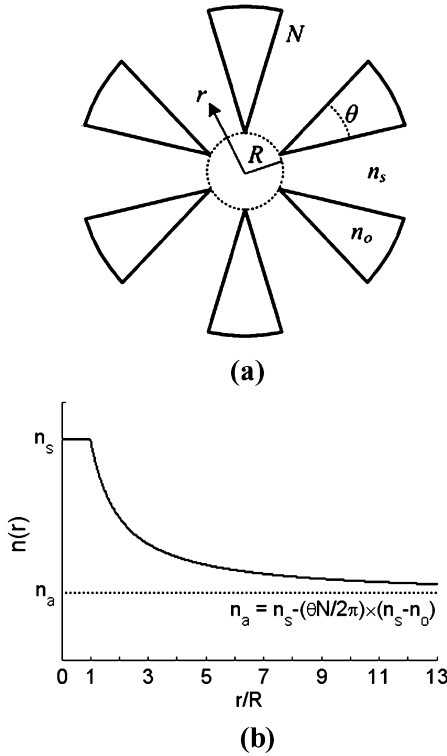


Fig. 1. (a) Schematic diagram of the holey wedge structure. Each of the N wedges is air-filled with index of refraction n_o , and the bulk semiconductor index of refraction is given by n_s . The optical aperture radius is given by R , and each arc subtends an angle of θ . (b) Wedge shape structure effective index profile plotted as a function of normalized radius r/R .

This equation for the approximate index of refraction profile provides three degrees of freedom (R , N , and θ) which can be designed and optimized for high single-mode performance. The approximation given in (1) is correct to within 1% for all choices of R , N , and θ used in this experiment. (1) is normalized to r/R and plotted in Fig. 1(b). This index of refraction profile is asymptotic for large r . The approximate value of the index asymptote is given by

$$n_a = n_s - \frac{\theta N}{2\pi}(n_s - n_o). \quad (2)$$

In practical designs, the wedges must have a finite length and, hence, r/R never becomes very large in the above equations. Consequently, the index profile of a practical device never closely reaches n_a . This asymptotic limit is still useful for comparing the effective index contrast of different designs.

Fig. 2(a) illustrates a cross-sectional schematic of an implant-confined holey VCSEL. The transverse index profile for the holey implant VCSEL and an un-etched implant VCSEL are drawn for comparison. The index contrast provided by the thermal lens [15] in the standard implant VCSEL is relatively weak compared to the index contrast of the etched wedges, provided the wedges have been etched sufficiently deep into the top DBR. This increase in index contrast should result in lowered diffraction loss in the device because the optical mode can be more tightly confined in the transverse direction.

To account for the effect of finite etch depth on the transverse index profile, a method which was originally described by Yok-

ouchi, *et. al.* in [8] for etched photonic crystal VCSELs is used as follows. A finite etching depth dependence factor γ (which ranges between 0 and 1) is calculated by determining the relative amount of the longitudinal optical mode which overlaps the pattern etched from the top VCSEL facet to a specified depth. The effective transverse index profile n_{eff} in the VCSEL is then calculated using a weighted average which accounts for the relative amount of optical mode present in the DBR layers which have been etched

$$n_{\text{eff}}(r) = (1 - \gamma)n_s + \gamma n(r). \quad (3)$$

This method of combining a proton-implant and etched holey structure to achieve single-mode VCSEL operation offers several advantages. First, the optical aperture diameter is no longer dependent on the other parameters of the design, and can be independent of the gain diameter. The optical aperture size is an independent degree of freedom. Second, the grading of the index can be tailored by varying the design parameters, as shown by (1). The inherent tradeoff between mode size and index contrast for single-mode operation in step-index designs (such as in small oxide aperture and photonic crystal approaches) is somewhat relaxed. By grading the index, a larger fundamental mode size can be supported for the same index contrast, which should allow greater single-mode output than possible with a step-index approach.

III. EXPERIMENT

Proton-implant confined holey VCSELs were fabricated as follows. A bottom n -type 36-period distributed Bragg reflector (DBR) consisting of alternating layers of $\text{Al}_{0.16}\text{Ga}_{0.84}\text{As}$ and $\text{Al}_{0.92}\text{Ga}_{0.08}\text{As}$, an undoped active region with five GaAs quantum wells, and a top p -type 21-period DBR, were grown by metalorganic vapor phase epitaxy with a designed operating wavelength of 850 nm. A backside contact (AuGe–Ni–Au) was deposited to form an ohmic contact to the n -type substrate, and top ring contacts (Ti–Au) were lithographically patterned and formed by liftoff after the metal deposition. Photoresist pillars in the center of each top ring contact served to mask and define the lasing apertures for the implant process. Protons were implanted at 330 keV with a dose of $4 \times 10^{14} \text{ cm}^{-2}$. Electron beam lithography was used to define the holey wedge patterns in polymethyl-methacrylate resist, and freon reactive ion etching (RIE) was used to transfer the pattern to an SiO_2 mask. Large isolation mesas were lithographically defined and similarly transferred to the SiO_2 mask. The isolation mesas and wedge-shaped holes were simultaneously etched into the top DBR using SiCl_4 –Ar inductively coupled plasma RIE, and freon RIE was used to remove the mask. Fig. 2(b) illustrates a scanning electron microscope image of a typical device after fabrication.

In this study, the ion implant aperture was fixed at $10 \mu\text{m}$ in diameter with $N = 7$ wedges patterned around the implant aperture. Each wedge was designed to be $5 \mu\text{m}$ long with a $\theta = 20^\circ$ arc length, and etched to a depth of approximately 15 DBR mirror periods. The overlap of the optical aperture diameter (R) with the implant aperture was varied from 0 to $4 \mu\text{m}$.

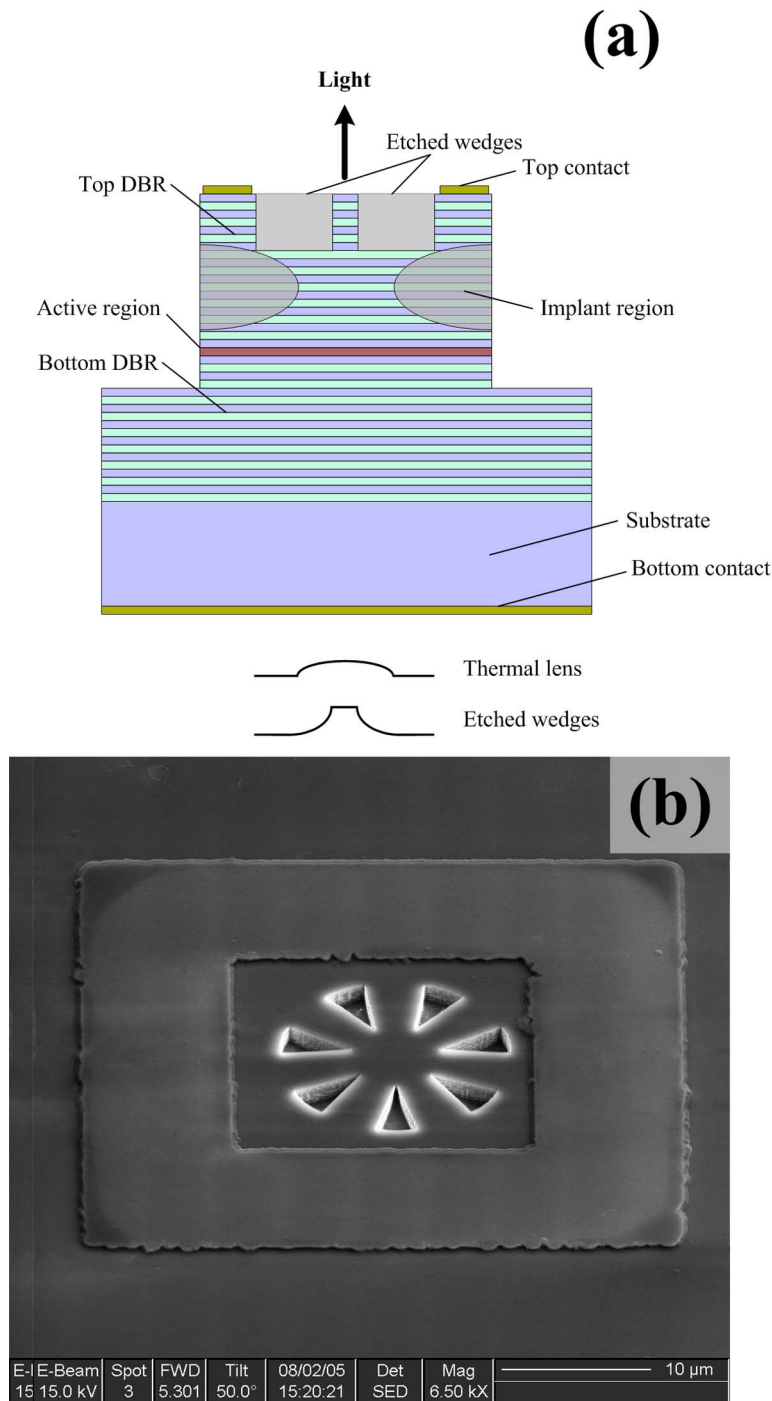


Fig. 2. (a) Cross-sectional schematic of an implant-confined VCSEL. The resulting index profiles are drawn (not to scale) for unetched implant and holey wedge implant VCSELS for comparison. (b) Scanning electron microscope image of a fabricated holey wedge implant VCSEL. (Color version available online at <http://ieeexplore.ieee.org>.)

The VCSEL characteristics were measured using on-wafer probing. For continuous wave (CW) light versus current ($L-I$) and current versus voltage ($I-V$) measurements, input current was varied and both the device voltage and the output from a silicon photodetector were measured using a semiconductor parameter analyzer. Pulsed $L-I$ measurements were obtained using a pulsed current source, and the output from the silicon photodetector was measured with a high-precision ammeter.

IV. RESULTS

Fig. 3(a) illustrates the optical spectra at maximum power for a single-mode device with an implant diameter of $10\ \mu\text{m}$. Single-mode operation is defined in this study for a side mode suppression ratio (SMSR) greater than 30 dB from threshold through rollover. Fig. 3(b) shows the CW $L-I$ characteristics for the same VCSEL (with design parameters $N = 7, R =$

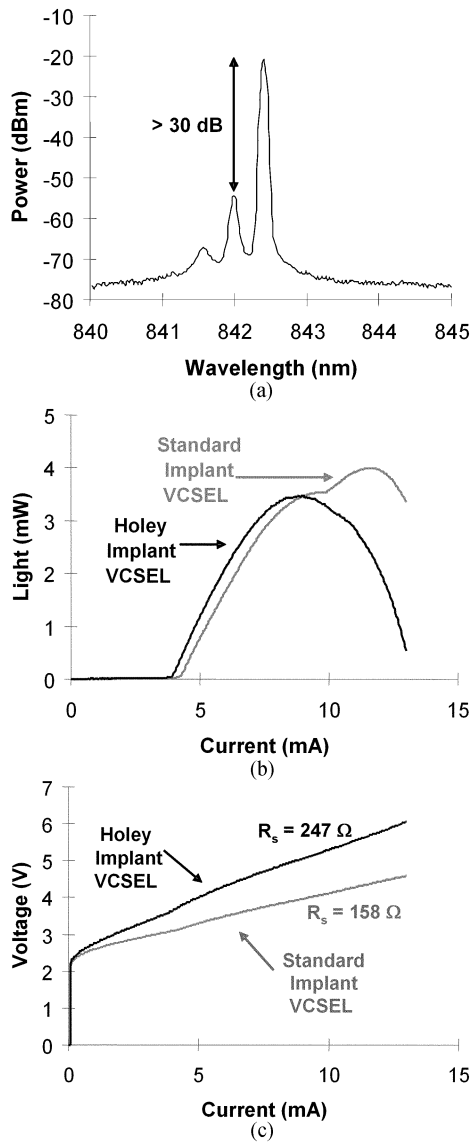


Fig. 3. (a) Spectrum at maximum output power of a single-mode holey wedge VCSEL with implant aperture of diameter $10 \mu\text{m}$. (b) CW $L-I$ characteristics and (c) CW $I-V$ characteristics of the same device. The $L-I$ of an unetched control device with the same size implant diameter is plotted for comparison.

$9 \mu\text{m}$, and $\theta = 20^\circ$), along with the characteristics for the control VCSEL which has no etched pattern. This control device exhibits a threshold of 4.2 mA with a maximum single-mode power of 3.25 mW , and becomes multimode at an injection level of 9.5 mA . After etching the wedge-shaped holey pattern, the threshold is reduced to 3.9 mA , and the single-mode output power increases to 3.5 mW , with single-mode operation being maintained to maximum power.

Fig. 3(c) illustrates the CW $I-V$ characteristics for the two VCSELs. The etched holes increase the series resistance of the laser compared to the unetched conventional device. This effect is likely due to the removal of the doped semiconductor material. The increase in series resistance may affect high-speed modulation of the etched VCSEL, since parasitics due to series resistance and capacitance often limit the maximum direct modulation rate.

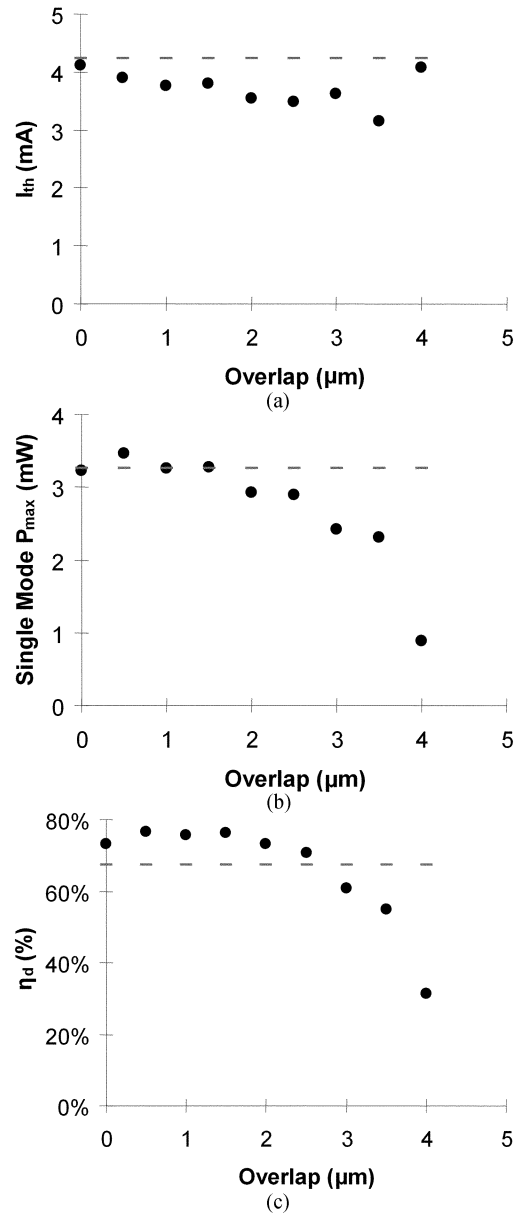


Fig. 4. (a) Threshold current, (b) maximum single-mode power, and (c) differential quantum efficiency as a function of overlap of the wedge tips with the implant aperture of diameter $10 \mu\text{m}$. The values for the unetched control device with the same implant aperture size have been plotted (dashed line) for reference.

The effect of the overlap of the wedge tip with the implant aperture region can also be characterized [13]. Fig. 4(a) illustrates the lasing threshold, Fig. 4(b) the maximum single-mode power, and Fig. 4(c) the differential quantum efficiency, all as a function of the overlap of the wedge tip with the proton-implant aperture region where lines have been included corresponding to the unetched control VCSEL with an implant aperture diameter of $10 \mu\text{m}$. In Fig. 4(a), the threshold current for every etched device is lower than that for the unetched control. As the overlap between the holey pattern and the implant aperture becomes greater, so does the reduction in net loss, which results in the decreasing threshold for increasing overlap trend. The fundamental mode suffers negligible loss for overlap distances less than $2 \mu\text{m}$, which is indicated in the preservation or

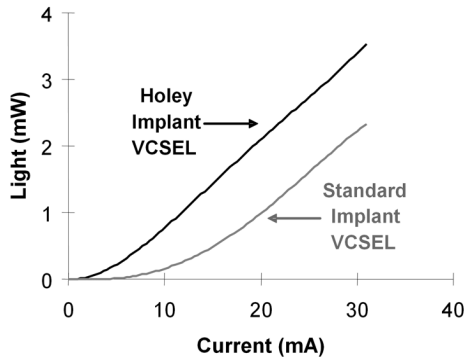


Fig. 5. Pulsed L - I characteristics of a holey wedge and unetched control VCSEL with implant aperture diameter $10\ \mu\text{m}$.

enhancement in single-mode output power shown in Fig. 4(b). The increase of the slope efficiency shown in Fig. 4(c) for devices whose tips penetrate less than $3\ \mu\text{m}$ is also consistent with reduced diffraction loss at threshold compared to proton implanted VCSELS. From these three figures it is apparent that optimal results are achieved when the wedges overlap the gain aperture defined by the implant by approximately $1.5\ \mu\text{m}$.

To inhibit the formation of a thermal lens and allow for direct observation of the optical confinement provided by the etched wedges, the injection current was pulsed with a period of $1\ \mu\text{s}$ and 10% duty cycle. Fig. 5 illustrates the pulsed L - I characteristics of the holey and conventional VCSELS. Under pulsed operation, the threshold current of the holey VCSEL was 3 mA compared to 8 mA for the unetched device. This large difference between pulsed threshold currents for the holey and conventional VCSELS indicates the etched wedges are providing sufficient index confinement to dominate the effect of thermal lensing. Note the threshold current for the holey VCSEL does not significantly change between CW and pulsed operation, indicating the thermally induced index plays no role at threshold.

Etching the holey structures has two significant effects on the optical properties of the VCSEL. First, the index profile of the etched wedges provides stronger index confinement which reduces the diffraction loss of the device. Second, the introduction of these holes increases the scattering and mirror loss in the region outside the designed optical aperture of radius R . If properly designed, this increased loss is selective to higher order modes. The decrease in CW threshold current evident in Figs. 3(b) and 5(a) indicates the total net loss of the holey VCSEL has been decreased compared to the conventional device. This implies the diffraction loss has been reduced by a greater amount than the increase in scattering loss due to the etched wedges. Additionally, the CW single-mode power for the fundamental mode was slightly increased. This increase is a result of the fundamental mode suffering negligible scattering loss due to the holes and gives an indication of the selectivity of fundamental mode scattering loss compared to higher order mode scattering loss.

Calculations using the derived index profile and the parameters used in this experiment show the modal cutoff condition for these etched designs are such that the index confinement could support multiple transverse modes. This suggests that mode

cutoff is not the primary mechanism for single-mode operation. Instead, single-mode operation is attributed to increased loss to the higher order modes. The fundamental mode also experiences a significant decrease in diffraction loss, resulting in a net reduction in total loss to the fundamental mode.

V. SUMMARY

Wedge-shaped holes have been designed, fabricated, and characterized in proton-implanted VCSELS. A model for the transverse index of refraction profile has been presented. Single-mode operation is attributed to increased loss to the higher order modes. CW and pulsed measurements indicate this holey structure can decrease threshold current, increase maximum single-mode output power, and increase the efficiency of the VCSEL. These improvements are found to be a direct result of a reduction in total loss to the fundamental mode and are caused by lowered diffraction loss due the optical confinement provided by the effective graded index profile which was introduced by the etched wedges. The fundamental mode size can be tailored through proper design of the graded index profile, with potential benefits including increased fiber coupling efficiency. Optimization of the hole shape could reduce the adverse effects on series resistance. With further refinement of the wedge-shape and implant diameter to form a more optimum radially graded index profile, greater enhancement of the single-mode VCSEL output is expected.

REFERENCES

- [1] C. Jung, R. Jäger, M. Grabherr, P. Schnitzer, R. Michalzik, B. Weigl, S. Müller, and K. J. Ebeling, "4.8 mW singlemode oxide confined top-surface emitting vertical-cavity laser diodes," *Electron. Lett.*, vol. 33, no. 21, pp. 1790-1791, 1997.
- [2] R. A. Morgan, G. D. Guth, M. W. Focht, M. T. Asom, K. Kojima, L. E. Rogers, and S. E. Callis, "Transverse mode control of vertical-cavity top-surface-emitting lasers," *IEEE Photon. Technol. Lett.*, vol. 4, no. 4, pp. 374-377, Apr. 1993.
- [3] E. W. Young, K. D. Choquette, S. L. Chuang, K. M. Geib, A. J. Fischer, and A. A. Allerman, "Single-transverse-mode vertical-cavity lasers under continuous and pulsed operation," *IEEE Photon. Technol. Lett.*, vol. 13, no. 9, pp. 927-929, Sep. 2001.
- [4] H. Martinsson, J. A. Vukusic, M. Grabherr, R. Michalzik, R. Jäger, K. J. Ebeling, and A. Larsson, "Transverse mode selection in large-area oxide-confined vertical-cavity surface-emitting lasers using a shallow surface relief," *IEEE Photon. Technol. Lett.*, vol. 11, no. 12, pp. 1536-1538, Dec. 1999.
- [5] H. J. Unold, S. W. Z. Mahmoud, R. Jäger, M. Kicherer, M. C. Riedl, and K. J. Ebeling, "Improving single-mode VCSEL performance by introducing a long monolithic cavity," *IEEE Photon. Technol. Lett.*, vol. 12, no. 8, pp. 939-941, Aug. 2000.
- [6] D. S. Song, S. H. Kim, H. G. Park, C. K. Kim, and Y. H. Lee, "Single-fundamental-mode photonic-crystal vertical-cavity surface-emitting lasers," *Appl. Phys. Lett.*, vol. 80, pp. 3901-3903, 2002.
- [7] N. Yokouchi, A. J. Danner, and K. D. Choquette, "Two-dimensional photonic crystal confined vertical-cavity surface-emitting lasers," *IEEE J. Sel. Topics Quantum Electron.*, vol. 9, no. 5, pp. 1439-1445, Sep. 2003.
- [8] N. Yokouchi, A. J. Danner, and K. D. Choquette, "Etching depth dependence of the effective refractive index in two-dimensional photonic-crystal-patterned vertical-cavity surface-emitting laser structures," *Appl. Phys. Lett.*, vol. 82, no. 9, pp. 1344-1346, 2003.
- [9] A. J. Danner, J. J. Raftery Jr., T. Kim, P. O. Leisher, A. V. Giannopoulos, and K. D. Choquette, "Progress in photonic crystal vertical cavity lasers," *IEICE Trans. Electron.*, vol. E88-C, no. 5, pp. 944-950, May 2005.
- [10] A. J. Danner, T. S. Kim, and K. D. Choquette, "Single fundamental mode photonic crystal vertical cavity laser with improved output power," *Electron. Lett.*, vol. 41, no. 6, pp. 325-326, 2005.

- [11] A. Furukawa, S. Sasaki, M. Hoshi, A. Matsuzono, K. Moritoh, and T. Baba, "High-power single-mode vertical-cavity surface-emitting lasers with triangular holey structure," *Appl. Phys. Lett.*, vol. 85, pp. 5161–5163, 2004.
- [12] H. P. D. Yang, F. I. Lai, Y. H. Chang, H. C. Yu, C. P. Sung, H. C. Kuo, S. C. Wang, S. Y. Lin, and J. Y. Chi, "Singlemode (SMSR > 40 dB) proton-implanted photonic crystal vertical-cavity surface emitting lasers," *Electron. Lett.*, vol. 41, no. 6, pp. 326–328, 2005.
- [13] P. O. Leisher, A. J. Danner, J. J. Raftery Jr., and K. D. Choquette, "Proton implanted single mode holey vertical-cavity surface emitting lasers," *Electron. Lett.*, vol. 41, no. 18, pp. 1010–1011, 2005.
- [14] K. D. Choquette and K. M. Geib, Wilmsen, Temkin, and Coldren, Eds., "Fabrication and performance of vertical-cavity surface-emitting lasers," in *Vertical-Cavity Surface-Emitting Lasers*. New York, : Cambridge Univ. Press, 1999, pp. 193–232.
- [15] N. K. Dutta, L. W. Tu, G. Hasnain, G. Zydzik, Y. H. Wang, and A. Y. Cho, "Anomalous temporal response of gain guided surface emitting lasers," *Electron. Lett.*, vol. 27, no. 3, pp. 208–210, 1991.



Paul O. Leisher (S'98) was born in Sao Paulo, Brazil, in 1980. He received the B.S. degree in electrical engineering from Bradley University, Peoria, IL. He received the M.S. degree in electrical engineering from the University of Illinois at Urbana-Champaign, in 2004, where he is currently working toward the Ph.D. degree, also in electrical engineering.

His research interests include design, fabrication, and characterization of photonic devices including photonic crystal and holey vertical-cavity surface-emitting lasers, photonic crystal light-emitting diodes, and photonic crystal emitters.

Mr. Leisher is a student member of the IEEE Lasers and Electro-Optics Society and the Optical Society of America.



Aaron J. Danner (S'98) was born in Maryville, MO, in 1977. He received the B.S. degree in electrical engineering from the University of Missouri-Columbia, in 2000, and the M.S. and Ph.D. degrees in electrical engineering from the University of Illinois at Urbana-Champaign, in 2002 and 2005, respectively.

In 2005, he joined Agilent Technologies, Singapore.

Dr. Danner is a member of the IEEE Lasers and Electro-Optics Society and the Optical Society of America.



James J. Raftery, Jr. (M'94) received the B.S. degree in electrical engineering from Washington University, St. Louis, MO, and his commission as an Officer in the United States Army in 1988. He received the M.S. degree from the University of Missouri-Columbia in 1996, and the Ph.D. degree from the University of Illinois at Urbana-Champaign in 2005, both in electrical engineering.

In 1996, he joined the faculty of the Department of Electrical Engineering and Computer Science at the United States Military Academy (USMA), West Point, NY. In 1999, he became the Power and Energy Research Program Manager at the Army Research Laboratory, Adelphi, MD. In 2001, he assumed duties as the Assistant Project Manager for Soldier Power, Fort Belvoir, VA, supporting the Army's Land Warrior program. In 2005, he returned to the electrical engineering faculty at USMA, where he is a Research Faculty Member in the Photonics Research Center. His research interests are in photonic crystal vertical-cavity surface-emitting lasers.

Dr. Raftery is a member of the IEEE/Lasers and Electro-Optics Society and the Optical Society of America.



Dominic F. Siriani received the B.S. degree in electrical engineering from the University of Illinois at Urbana-Champaign in 2006, where he is currently working toward the M.S. degree.

His research interests include design, fabrication, and characterization of vertical-cavity surface-emitting lasers.



Kent D. Choquette (M'97–F'03) received the B.S. degree in engineering physics and applied mathematics from the University of Colorado, Boulder, in 1984, and the M.S. and Ph.D. degrees in materials science from the University of Wisconsin-Madison, in 1985 and 1990, respectively.

In 1990, he held a postdoctoral appointment at AT&T Bell Laboratories, Murray Hill, NJ. In 1992, he joined Sandia National Laboratories, Albuquerque, NM, as a Postdoctoral Researcher, and in 1993, as a Principal Member of Technical Staff. He became a Professor in the Electrical and Computer Engineering Department, University of Illinois at Urbana-Champaign in 2000, and in July 2005 became the acting Director of the Micro and Nanotechnology Laboratory. His Photonic Device Research Group is centered around the design, fabrication, characterization, and applications of vertical-cavity surface-emitting lasers (VCSELs), novel microcavity light sources, nanofabrication technologies, and hybrid integration techniques. From 2000 to 2002, he was an IEEE/Lasers and Electro-Optics Society (LEOS) Distinguished Lecturer. He has authored more than 200 technical publications and three book chapters, and has presented numerous invited talks and tutorials on VCSELs.

Dr. Choquette has served as an Associate Editor of the IEEE JOURNAL OF QUANTUM ELECTRONICS and IEEE PHOTONIC TECHNOLOGY LETTERS, and as a Guest Editor of IEEE JOURNAL OF SELECTED TOPICS IN QUANTUM ELECTRONICS. He is a Fellow of both the IEEE Lasers and Electro-Optics Society and the Optical Society of America.